Environmental Science & Technology

Article

Cite This: Environ. Sci. Technol. 2019, 53, 8845−8853

pubs.acs.org/est

Impacts of SO_2, Relative Humidity, and Seed Acidity on Secondary Organic Aerosol Formation in the Ozonolysis of Butyl Vinyl Ether

Peng Zhang,[†,§] Tianzeng Chen,[†,§] Jun Liu,[†,§] Changgeng Liu,[†] Jinzhu Ma,[†,‡,§] Qingxin Ma,[†,‡,§] Biwu Chu,[†,‡,§] and Hong He*[,†,‡,§]

[†]State Key Joint Laboratory of Environment Simulation and Pollution Control, Research Center for Eco-Environmental Sciences, Chinese Academy of Sciences, Beijing 100085, China

[‡]Center for Excellence in Regional Atmospheric Environment, Institute of Urban Environment, Chinese Academy of Sciences, Xiamen 361021, China

[§]University of Chinese Academy of Sciences, Beijing 100049, China

Supporting Information

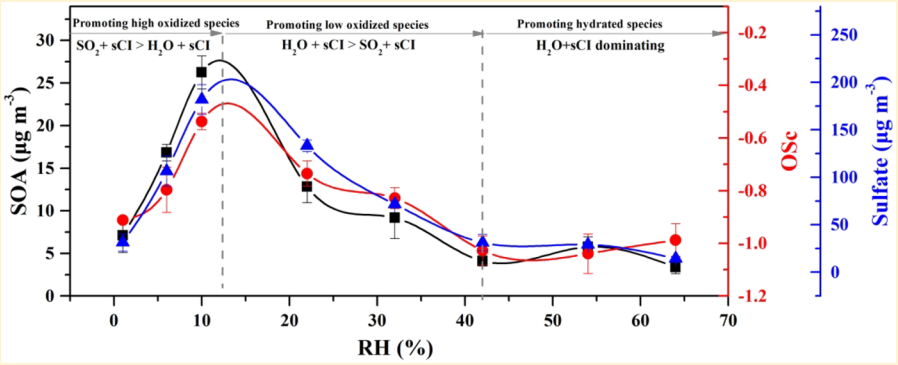

ABSTRACT: Alkyl vinyl ethers are widely used as fuel additives. Despite this, their atmospheric chemistry and secondary organic aerosol (SOA) formation potentials are still not well-known under complex pollution conditions. In this work, we examined the impact of SO_2, relative humidity (RH), and particle acidity on the formation and oxidation state (OSc) of SOA from butyl vinyl ether (BVE) ozonolysis. Increasing SO_2 concentration produced a notable promotion of SOA formation and OSc due to the significant increase in H_2SO_4 particles and formation of more highly oxidized components. Increased RH in the presence of SO_2 appeared to promote, suppress, and dominate the formation and OSc of SOA in the dry range (1−10%), low RH range (10−42%), and moderate RH range (42−64%), respectively. This highlights the importance of competition between H_2O and SO_2 in reacting with the stabilized Criegee intermediate in BVE ozonolysis at ambient RH. Increased particle acidity mainly contributed to the change in chemical composition of BVE-dominated SOA but not to SOA formation. The results presented here extend previous analysis of BVE-derived SOA and further aid our understanding of SOA formation potential of BVE ozonolysis under highly complex pollution conditions.

INTRODUCTION

Secondary organic aerosol (SOA) represents a substantial fraction of atmospheric submicron particles.[1−3] However, simulated SOA concentrations often dramatically underestimate observed values, especially in polluted regions.[4−7] Inadequate precursor emission databases and unknown chemical mechanisms may be potential contributors to these discrepancies.[4,8]

Recently, oxygenated volatile organic compounds (OVOCs) have become recognized as a class of potential contributors to SOA formation. Extensive studies have shown that liquid-phase oligomerization reactions of saturated OVOCs (i.e., glyoxal, methylglyoxal, and propanal) are an important pathway promoting SOA formation and also play an important role during haze formation in polluted urban areas.[9−12] As one subset of OVOCs, however, studies on the contribution of unsaturated OVOCs to ambient SOA formation remain limited.

Among unsaturated OVOCs, alkyl vinyl ethers are increasingly produced in the chemical industry and widely used as fuels and fuel additives. Compared with the corresponding alkenes, alkyl vinyl ethers show high reactivity toward atmospheric oxidants (OH, NO_3, and O_3) due to an activating effect of the ether group (−O−) on the C═C double bond.[13] To assess their lifetimes and roles in tropospheric chemistry, the degradation mechanisms and kinetics of the gas-phase reactions of these alkyl vinyl ethers

Received: May 5, 2019
Revised: July 8, 2019
Accepted: July 12, 2019
Published: July 12, 2019

DOI: 10.1021/acs.est.9b02702
Environ. Sci. Technol. 2019, 53, 8845−8853

toward OH, NO_3, and O_3 have been widely studied using smog chambers.[14−18] To date, however, only three studies on SOA formation of alkyl vinyl ethers have been reported. The study from Klotz et al. showed that ozonolysis of methyl vinyl ether can produce a significant amount of SOA, but not OH or NO_3 radical reactions.[14] In addition, Sadezky et al. further proved that oligoperoxides produced by repeated peroxy radical-stabilized Criegee intermediate (sCI) addition are crucial SOA components in the absence of SO_2.[19,20] More recent studies have also reported that anthroponotic emissions have a significant impact on SOA formation.[21−24] For example, the homogeneous reaction between SO_2 and sCI is widely considered to be an important source of both atmospheric sulfate and SOA.[25−27] The multiphase reaction between SO_2 and organic peroxides from alkene ozonolysis has also been proposed as an important source of organosulfates contributing to SOA growth.[21,28,29] Therefore, butyl vinyl ether (BVE) ozonolysis in the atmosphere needs to be considered more realistically. To assess the potential capacity of alkyl vinyl ethers to generate SOA under highly complex pollution conditions, a better understanding of the atmospheric chemistry of this class of unsaturated OVOCs is therefore highly desirable.

In this work, we used an aerodyne high-resolution time-of-flight aerosol mass spectrometer (HR-ToF-AMS) to examine the chemistry of SOA generated from the ozonolysis of BVE over a wide range of SO_2 concentrations and relative humidity (RH). This study aimed to provide a profound understanding of the atmospheric ozonolysis process of BVE and SOA formation under complex pollution conditions by investigating the impact of SO_2, RH, and particle acidity on BVE-dominated SOA.

■ EXPERIMENTAL METHODS

The experiments were conducted in a 30 m^3 stainless steel, fixed-volume chamber with 125 μm Teflon coated walls. The chamber has been described in detail in our recent works.[24,29] All experiments were carried out in the dark at a constant temperature (24−25 °C). Prior to each experiment, the Teflon-coated chamber was flushed with clean, dry air for 24 h until the particle concentration was < 50 cm^{-3} and volume concentration was < 0.01 μm^3 cm^{-3}. The experimental purposes and reaction conditions for the experiments were listed in Table S1. To prevent reactions of BVE with OH radicals generated during ozonolysis of BVE, CO (∼35 ppm) was used as an OH scavenger and added to the chamber. The sequence of reactants entering the chamber was as follows: water/seed particles, ozone, SO_2, CO, and finally BVE. Nonacidified and acidified ammonium sulfate seed aerosols were generated by nebulizing aqueous solutions of 0.02 M $(NH_4)_2SO_4$ (AS, aq) and 0.02 M $(NH_4)_2SO_4$ (aq) + 0.02 M H_2SO_4 (AAS, aq), respectively. After completing the injection, the seed aerosols were allowed to stabilize for approximately 20 min in the chamber. However, it should be noted that a diffusion dryer was placed after the atomizer to remove liquid water from the seed particles and eliminate its influence on the volume/mass concentration of seed particles. Water vapor was generated using a 500 mL stainless steel bubbler placed before the chamber inlet. Ozone was generated by passing synthetic air (4 L min^{-1}) through an ozone generator composed of a quartz cell and mercury Pen-Ray lamp with a metal aluminum foil cover. Both SO_2 (520 ppm in N_2, Beijing Huayuan Gas Company, China) and CO (0.02% in N_2, Beijing Huayuan Gas Company, China) were subsequently injected into the chamber directly through flow controllers to target concentrations. After a 10 min mixing period, 20 μL of BVE was injected with a microsyringe into a heated stainless-steel "tee" fitting (80 °C) where it vaporized and was then flushed into the chamber rapidly by dry dilution air flow with a flow rate of 15 L min^{-1}.

A suite of instruments was used to investigate gas- and particle-phase chemistry. Here, O_3, SO_2, CO, and NO_x were continuously monitored using a Model-49i O_3 analyzer (Thermo Fisher Scientific Inc.), Model-43i SO_2 analyzer (Thermo Fisher Scientific Inc.), Model-48i CO analyzer (Thermo Fisher Scientific Inc.), and Model-42i-TL NO_x analyzer (Thermo Fisher Scientific Inc.), respectively.[30] Real-time aerosol spectra were collected by HR-TOF-AMS.[31,32] The AMS switched once every 2 min between the high-resolution "W mode" and lower resolution, higher sensitivity "V mode". AMS measurements can provide information about SOA composition in detail, such as the bulk aerosol H/C and O/C ratios along with the average aerosol carbon oxidation state (OSc), and temporal evolution of both sulfate and SOA. Aerosol size distribution, volume, and total number and mass concentrations were measured with a scanning mobility particle sizer (SMPS), consisting of a differential mobility analyzer (DMA; Model 3082, TSI Inc.) and a condensation particle counter (CPC; Model 3776, TSI, Inc.). The operating conditions for the SMPS were 0.3 L min^{-1} sample flow, 3 L min^{-1} sheath flow, and 19−700 nm size scan. Particle mass concentrations were corrected according to the decay of ammonium sulfate mass due to the presence of particle wall loss. The wall loss rate of AS particles was in accordance with $k_{dep} = 4.15 \times 10^{-7} \times D_p^{1.89} + 1.39 \times D_p^{-0.88}$ (where D_p is the particle diameter (nm))[33] according to the method in Takekawa et al.[34] To verify experimental reproducibility, parallel experiments under all conditions were conducted in the chamber (Figure S1).

■ RESULTS AND DISCUSSION

Effects of SO_2 on SOA Formation and Composition. China has the highest concentration of SO_2 in the world due to the large proportion of energy supply coming from coal combustion.[35] Notably, high concentrations of SO_2 ranging from 40 ppb to over 100 ppb are still frequently observed during winter in certain regions of China.[36,37] Therefore, investigating the effects of different SO_2 levels on the formation and composition of BVE SOA is very necessary. In the current study, the initial SO_2 mixing ratios ranged from 0 to 127 ± 3 ppb in the SO_2 experiments.

Figure 1A shows SOA formation as a function of time in the absence and presence of SO_2 under seed-free conditions. Compared with that in the absence of SO_2, the presence of SO_2 promoted significant formation of SOA. More importantly, both sulfate and SOA markedly increased with increased SO_2 concentration, as shown in Figure 1B. In addition, given that O_3 concentration tended to be steady with reaction time (Figure S2), BVE was oxidized completely in the presence of excess O_3. Furthermore, we estimated SOA yield (Y), defined as $Y = \Delta M_0/\Delta BVE$, which was also found to increase with the increase in SO_2. The significant increase in sulfate implies that elevated SO_2 greatly promoted the reaction of SO_2 with sCI formed during the ozonolysis of BVE and subsequently led to more H_2SO_4 particle formation. Accompanied by the formation of H_2SO_4 particles, more components containing

DOI: 10.1021/acs.est.9b02702
Environ. Sci. Technol. 2019, 53, 8845−8853

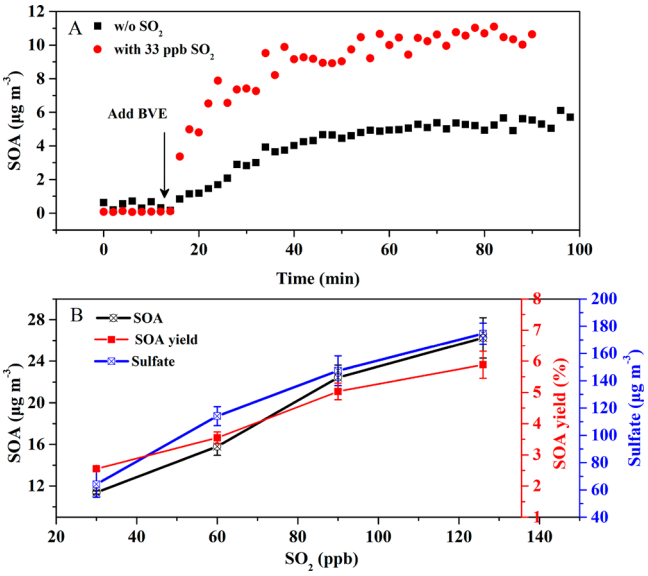

Figure 1. (A) SOA formation as a function of reaction time in the absence and presence of SO_2. (B) Formation of sulfate and SOA and SOA yield as a function of SO_2 concentration.

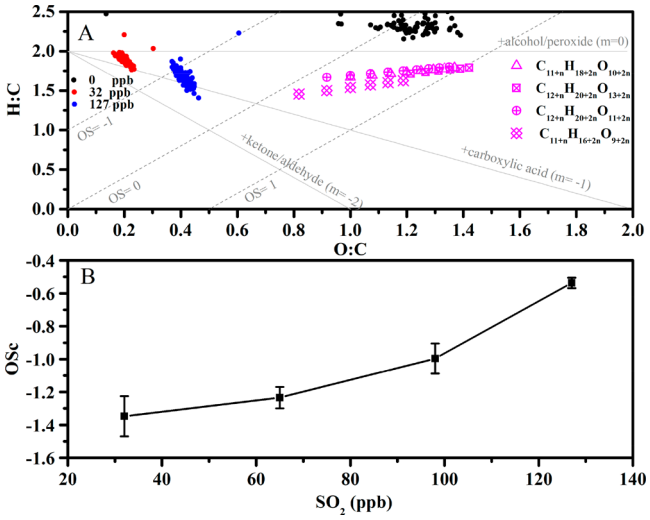

Figure 2. (A) Van Krevelen plots of BVE SOA in the presence of 0, 32, and 127 ppb SO_2. Pink marker indicates O/C and H/C values of different oligomer series characterized by Sadezky et al.[19] (B) SOA OSc as a function of SO_2 concentration.

aldehyde or carbonyl groups could be produced after the reaction between sCI and SO_2, as based on previous work.[21,38,39] These aldehyde and carbonyl species could further react with other species, such as components with aldehyde (−CHO), hydroxy radical (−OH), or peroxyhydroxy radical (−OOH) groups to form dimers or oligomers via aldol condensation, hemiacetal formation, and the hydroperoxide pathway.[38] The formation of dimers or oligomers can further contribute to SOA formation and growth.[38,40] Thus, one crucial reason for the enhanced effect of SO_2 on SOA formation is that more H_2SO_4 particles provide a higher surface area and volume for condensation of low-volatility oxidized species.[41−43] Both the increase in number concentration of secondary particles with the increase of SO_2 concentration (Figure S3) and the higher concentration of sulfate from the size-resolved distribution of sulfate relative to SOA (Figure S4) support the above conclusion.

Additionally, both composition and chemical evolution of SOA in the absence and presence of SO_2 were compared on the basis of the H/C vs O/C plot. The slope of a fitted line in a Van Krevelen diagram can be used to infer the composition of SOA and the chemical processes in SOA formation.[44−46] As shown in Figure 2A, the overall regions of experimental data were noticeably different between experiments with and without SO_2. The O/C and H/C ratios of SOA without SO_2 were both noticeably higher than those in the presence of SO_2. In particular, the H/C of SOA (2−2.5) in the absence of SO_2 was higher than that of BVE (H/C = 2) and almost stable, whereas the H/C ratio in the presence of SO_2 was noticeably lower and rapidly decreased as the reaction progressed. These differences were mainly caused by different reaction mechanisms. In the absence of SO_2, the overall O/C observed in the current study is in agreement with the O/C ratio of oligoperoxides characterized by Sadezky et al.[19,20] The slope of zero was attributed to the addition of alcohol or peroxide functional groups to the carbon backbone. This further reinforces previously reported results showing that oligoperoxides formed through the oligomerization pathway of sCI account for the majority of BVE-derived SOA in the absence of SO_2.[19,20] For the case with SO_2, the evolution of SOA composition was generally consistent with the classical path that O/C increases when H/C decreases.[47] As the data resulted in a Van Krevelen slope steeper than −2 in Figure 2, this suggests the substantial addition of ketone or aldehyde. One potential explanation for the steeper slope is that certain condensed-phase reactions may alter the nature of the functional groups comprising SOA or the volatility of particulate compounds.[45] For example, dehydration reactions, such as esterification, aldol condensation, and cyclization, which involve the loss of water molecules, can shift the Van Krevelen slope toward steeper values.[48] The decrease in the O/C ratio resulting from the dehydration reaction may partially offset the overall increase in the O/C ratio. As a result, the O/C ratio did not manifest a significant increase with the rapid decrease in the H/C ratio in the particle phase.

Average OSc, defined as OSc = 2 × O/C − H/C, is considered an effective indicator of atmospheric oxidative aging processes.[49,50] Thus, OSc was employed to assess the oxidation degree of organic species in all experiments. The OSc was calculated using the O/C and H/C ratios obtained in the stable stage of SOA. As shown in Figure 2B, SOA OSc noticeably increased with increasing SO_2. One potential explanation for this phenomenon is that several more highly oxidized products were formed at the higher SO_2 levels due to the higher O/C ratio in the presence of 127 ppb SO_2 relative to that in the presence of 32 ppb SO_2. The results are consistent with those reported by Ye et al.,[21] who suggested that the increase in sulfur-containing compounds produced via functionalization was mainly responsible for the higher OSc of products from limonene ozonolysis in the presence of SO_2. As shown in Figure S5, the higher initial concentration of SO_2 resulted in a higher S/C ratio of SOA. This not only indicates the presence of organic sulfates in this study, but suggests that a higher initial SO_2 concentration will support more organosulfate formation given that organosulfate yield is reported to be positively correlated with the concentration of SOA and sulfate.[29,51] Thus, in the current study, the formation of more highly oxidized compounds (such as organosulfate) via

DOI: 10.1021/acs.est.9b02702
Environ. Sci. Technol. 2019, 53, 8845−8853

functionalization at higher SO_2 levels can be considered a crucial factor promoting the increase in the OSc of SOA.

Effects of Relative Humidity on SOA Formation and Composition. Water is ubiquitous in the atmosphere, and therefore, any chemical reaction or physical process involving water as a reactant, product, or solvent may be affected by humidity. Relative humidity (RH) has been reported to have a significant impact on new particle formation, chemical composition, and physical properties of SOA.[52−54]

To further understand the role of water in the ozonolysis of BVE, we expanded the SO_2 experiment to incorporate additional humidity conditions. SOA formation was measured under RH values of 1−64% in the presence of ∼125 ppb SO_2. As shown in Figure 3A, the change in SOA formation with RH

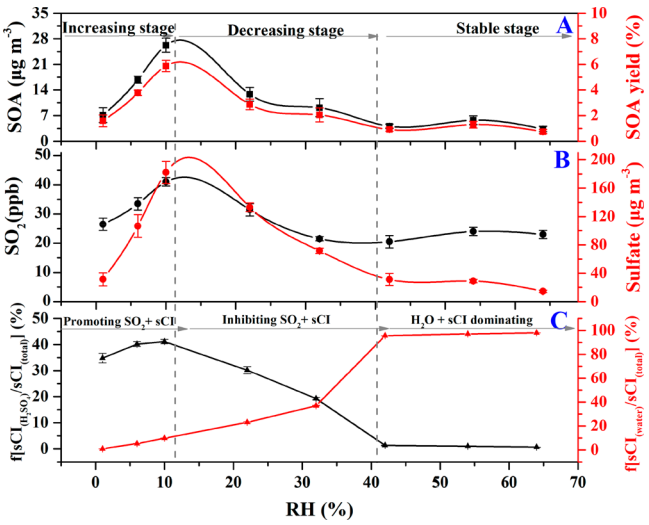

Figure 3. (A) SOA formation and yield during BVE ozonolysis as a function of RH. (B) Sulfate formation and SO_2 consumption as a function of RH. (C) Fractions of sCI that reacted with SO_2 and water as a function of RH.

could be divided into three stages: i.e., increasing, decreasing, and stable. In the increasing stage, with the initial RH increasing from 1 to 10%, SOA increased by over a factor of 2. During the decreasing stage, however, the increase in low RH (10−42%) reduced SOA formation. Conversely, SOA formation tended to be stable at moderate RH (42−64%). The changes in both sulfate formation and SO_2 consumption with RH were in line with that of SOA formation (Figure 3B). As the surface area and volume of sulfate particles are closely related to SOA formation, the difference in evolution of SOA in different RH ranges could be mainly ascribed to the promoting or inhibiting effects of water on the formation of sulfate particles. In the dry range (< 10%), the reaction rate constant of SO_2 and sCI is reported to be at least 4 orders of magnitude higher than the reaction rate constant of H_2O and sCI,[54] and the increase in RH can profoundly enhance the nucleation and growth of H_2SO_4 particles.[55,56] Thus, the promotion effect of water on SOA formation in the dry range (< 10%) could be explained by the increase in water vapor in the chamber significantly enhancing the formation of sulfuric acid particles, thus providing a higher surface area for condensation. In contrast, further increases in RH hindered the formation of H_2SO_4 particles when sCI consumption resulting from reactions with water and water dimer became more competitive with increasing RH (10−42%). Another plausible reason for the suppression of SOA mass loading is that the presence of a significant amount of water vapor may affect the production rate of SOA and favor the formation of lower molecular weight volatile oligomers by altering the formation mechanism of SOA.[57,58] After RH exceeded 42%, the changes of SOA and sulfate formation along with SO_2 consumption were negligible. One possible explanation is that the reaction between sCI and water or water dimer dominated SOA formation at the moderate RH range (> 42%) and partitioning equilibrium of low-volatility oligomers may occur when sCI is consumed completely by water or water dimers.[59,60] During new particle formation in the initial reaction period, SO_2 showed a negligible change in the high RH range (Figure S6). This implies that the impact of the reaction between SO_2 and sCI on initial particle formation can be neglected and other unidentified mechanisms may dominate the sink of SO_2 and sulfate formation as the reaction progresses. Ye et al. stated that the aqueous reaction between SO_2 and organic peroxides from monoterpene ozonolysis is a dominant sink of SO_2 at 50% RH.[21] Thus, it is plausible that the aqueous reaction of SO_2 with organic peroxides may also be the dominant source of sulfate in BVE ozonolysis when RH exceeded 42%. A previous study has shown that aqueous-phase SO_2 can react with dissolved ozone at appreciable rates at high pH.[61] Recently, however, Ye et al. further proved that the effect of 6 h reactions between SO_2 (289 ppb) and O_3 (485 ppb) either in the gas or particle phase on SO_2 consumption is negligible under 50% RH.[21] Thus, we concluded that reactions between SO_2 and O_3 also had negligible effects on SO_2 consumption due to the lower concentration of SO_2 (125 ppb) and O_3 (200 ppb) and the shorter reaction time (<2.5 h) employed in this work.

Moreover, we also applied a simplified model to quantitatively demonstrate the importance of the competitive reactions of sCI + H_2O and sCI + SO_2 to better understand the nonlinear behavior of sulfate and SOA with the increase in RH in a clear and logical manner. Kinetic model reactions of BVE ozonolysis in the presence of SO_2 are shown in Scheme 1. The kinetic parameters of the simplest sCI (CH_2OO) summarized in Table S2 were used in the simulation.

The fractions of sCI that reacted with SO_2 and with water as a function of RH were modeled according to the following equations.[62,63]

Scheme 1. Kinetic Model Reactions of BVE Ozonolysis in the Presence of SO_2

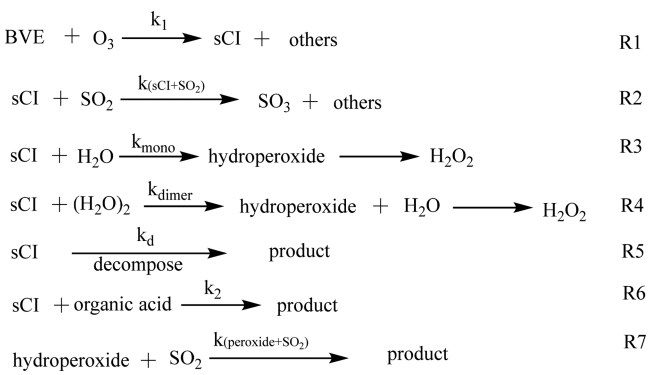

DOI: 10.1021/acs.est.9b02702
Environ. Sci. Technol. 2019, 53, 8845−8853

$$\frac{sCI_{SO_2}}{sCI_{tot}} = \frac{1}{1 + \frac{k_{mono}[H_2O] + k_{dimer}[(H_2O)_2] + k_d}{k_{(sCI+SO_2)}[SO_2]}} \quad (1)$$

$$\frac{sCI_{water}}{sCI_{tot}} = \frac{1}{1 + \frac{k_{(sCI+SO_2)}[SO_2] + k_d}{k_{mono}[H_2O] + k_{dimer}[(H_2O)_2]}} \quad (2)$$

where $k_{(sCI+SO_2)}$, $k_{(sCI+H_2O)}$, $k_{(sCI+(H_2O)_2)}$, and k_d are the reaction rate constants of sCI with SO_2, water monomer, water dimer, and other species, respectively; $[SO_2]$, $[H_2O]$, and $(H_2O)_2$ are the concentrations of SO_2, water monomer, and water dimer, respectively; and sCI_{SO_2}, sCI_{water}, and sCI_{tot} are the concentrations of sCI that oxidize SO_2, water, and total formed sCI, respectively.

The concentration of water dimer was calculated using the following equation:[64]

$$[(H_2O)_2)] = 1.23 \times 10^{15}\left(\frac{RH}{100\%}\right)cm^{-3} \quad (3)$$

As expected, the fractions of sCI that oxidized SO_2 exhibited similar variation trends over the RH range (Figure 3C), demonstrating that the change in RH indeed had an impact on sulfate formation from the reaction of sCI and SO_2. With the increase in RH, the fractions of sCI that reacted with water increased continually. For example, for RH > 32%, more than 95% of sCI reacted with water vapor, consistent with that reported by Berndt et al.[65]

To better illustrate the possible effects of RH on SOA composition, the change in OSc as a function of RH is shown in Figure 4A. The same as SOA formation, OSc also exhibited

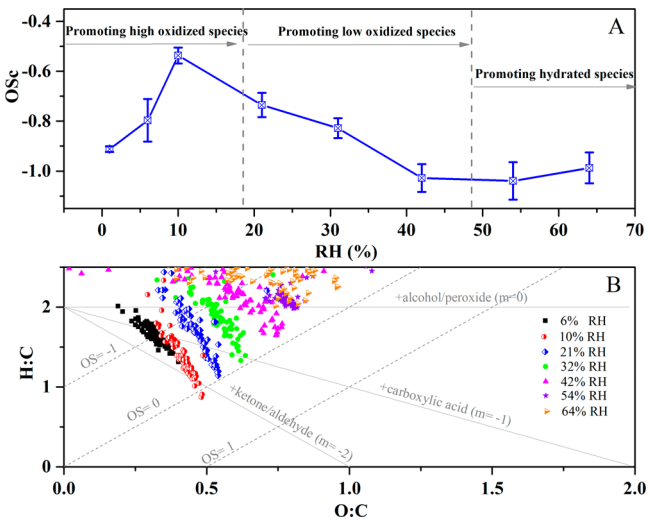

Figure 4. (A) SOA OSc as a function of RH. (B) Van Krevelen plots of BVE-derived SOA at RH ranging from 1% to 64%.

a similar variation trend over the RH range. Based on the Van Krevelen diagrams in Figure 4B, the O/C ratio of SOA at 10% RH was higher than that at 6% RH. This indicates that the increase in water vapor noticeably promoted the formation of more highly oxidized components compared with the dry range, leading to an increase in OSc. In contrast, further increases in RH in the low RH range markedly reduced SOA OSc due to the formation of less oxidized components with relatively higher H/C ratios, such as the H/C ratio at 32% RH. Another possible reason for this phenomenon is that more volatile oligomers with lower molecular weight were formed with increased RH, which did not condense significantly on particles during BVE ozonolysis, leading to a decrease in OSc with RH, like the effect of RH on the SOA components of isoprene.[66] When RH exceeded 42%, the higher H/C and O/C ratios of SOA observed in the moderate RH range relative to BVE (H/C = 2) suggest that hydration reactions may have dominated the formation of the majority of SOA components. The lower reactivity of hydrated species or oligomers toward O_3 may also have resulted in the negligible change observed in OSc in the moderate RH range.

Based on the above data, it could be concluded that RH had an impact on the formation and chemical composition of BVE-derived SOA, consistent with several recent studies.[52,67] The change in sulfate concentration resulting from the competitive reaction between SO_2 and H_2O toward sCI was a crucial factor influencing the change in SOA formation and OSc under the dry and low RH ranges. Additionally, the aqueous reaction of SO_2 with organic peroxides may be one possible factor dominating sulfate formation in the high RH range. However, it would be very difficult to estimate the relative contribution of sCI vs aqueous pathways in sulfate formation utilizing only the HR-TOF-AMS data in this work. Future research should focus on the role of peroxide from BVE ozonolysis systems in oxidizing SO_2 under atmospheric-related RH and should assess the atmospheric importance of these reactions as a SO_2 sink.

Effects of Seed Particles on SOA Formation. Many studies have shown that the acidity of seed particles has a profound impact on SOA formation.[68−71] To further elaborate the effect of seed acidity on SOA formation in the presence of SO_2, we examined the relationship between aerosol formation and seed particles with different acidity, including AS (weak-acidity) and AAS (acidic). Prior to the injection of BVE, the seed concentration and particle size distributions of AS and AAS in the chambers were similar (Figure S7). Formed gaseous H_2SO_4 and oxidation products simultaneously contributed to new particle formation via homogeneous nucleation (Figure 5). Moreover, the increase in seed particle size after addition of BVE could also be attributed to the condensation of newly fomred H_2SO_4 and oxidation products into pre-existing seed particles (Figure S7). It is worth noting that the concentration of new particles observed for the weak-acidic seeds was more than four times greater than that for acidic seeds. The greater adsorption of BVE on the AAS surface, relative to AS (Figure S8), supports the supposition that an increase in particle acidity can significantly enhance the uptake of BVE on particle surfaces (just like monoterpenes), thus reducing the particle concentration in the initial reaction period.[72] In addition, the higher concentration of particles observed for NaCl seeds further supports the above conclusion (Figure S9). However, the lower concentration of particles resulting from the increase in particle acidity did not lead to a decrease in either SOA or sulfate (Figure 6A). Thus, it can be speculated that heterogeneous reactions of O_3 and particulate BVE may be another important SOA and sulfate pathway in the presence of acidic seeds.[72] Moreover, OSc and O/C were both noticeably higher in the presence of AAS than in the presence of AS (Figure 6B). It is likely that the acidic seeds tended to readily promote the formation of more highly oxidized products via functionalization reactions relative to oligomerization reactions in BVE ozonolysis, even if acidic sulfate can simultaneously promote both functionalization and oligomerization reactions.[73,74] This provides further evidence

DOI: 10.1021/acs.est.9b02702
Environ. Sci. Technol. 2019, 53, 8845−8853

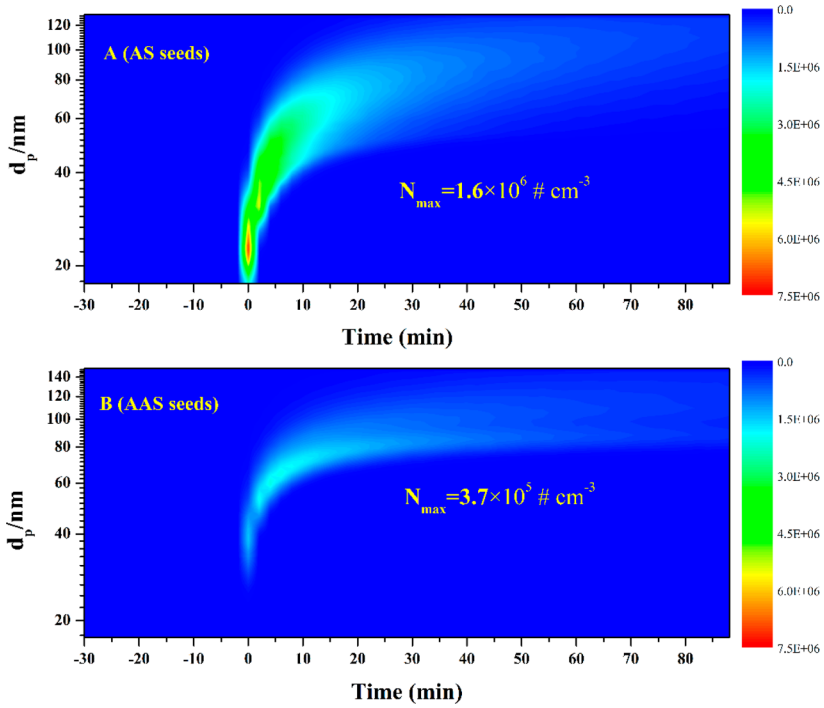

Figure 5. Size distributions of suspended particles as a function of time during ozonolysis of BVE/SO_2 in the presence of AS and AAS seed particles. N_{max} shows the maximal particle concentration during the reaction for each experiment.

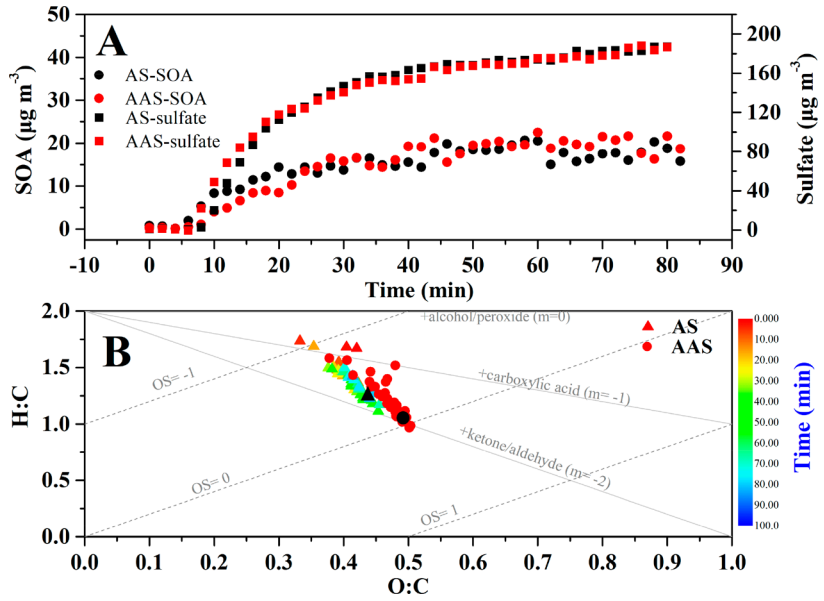

Figure 6. (A) SOA and sulfate formation during BVE ozonolysis in the presence of AS and AAS seed aerosols. (B) Van Krevelen plots of BVE-derived SOA with AS and AAS seed aerosols. Black markers indicate mean O/C and H/C values of SOA with AS (triangle) and AAS (circle).

that particle acidity mainly contributed to the change in the chemical composition of BVE-derived SOA.

■ ATMOSPHERIC IMPLICATIONS

Building upon previous studies on the ozonolysis of BVE, we further investigated the effects of SO_2, RH, and seed acidity on the formation and oxygenation degree of BVE-derived SOA. The increase in initial SO_2 concentration not only significantly promoted SOA formation but increased the particle oxidation state. By directly observing the changes in the formation and OSc of SOA under varied RH, we demonstrated that different reaction mechanisms dominated SOA formation in different RH ranges. In the dry range (1−10%), the sCI + SO_2 reaction grew in importance, which not only provided greater surface area and volume for condensation of low-volatility oxidized species by producing more H_2SO_4 particles but also promoted the formation of more highly oxidized products. In the low RH range (10−42%), the sCI + H_2O reaction became more important with the increase in RH. The decrease in sulfate and formation of less oxidized products were responsible for the decrease in SOA and OSc. When RH exceeded 42%, no further significant changes in SOA formation or OSc were observed

DOI: 10.1021/acs.est.9b02702
Environ. Sci. Technol. 2019, 53, 8845−8853

with elevated RH. This indicates that the oligomerization reaction of hydrated carbonyl in the aqueous phase may dominate SOA formation. Additionally, increased acidity was found to have a negligible effect on SOA formation but noticeably promoted SOA OSc. This suggests that particle acidity contributed substantially to the change in chemical composition but not SOA formation.

This work has important implications for further understanding the atmospheric oxidation of BVE and its SOA formation potential. Our findings imply that in highly polluted regions BVE is an important potential contributor to the formation of sulfate and SOA under atmospherically relevant RH, SO_2, and O_3 concentrations. Given the vast array of unsaturated OVOC species present in the atmosphere of both biogenic and anthropogenic origin, it is likely that similar effects of SO_2, RH, and particle acidity also occur during the ozonolysis of other unsaturated OVOCs in the atmosphere. The results observed in this study provide new insights into SOA formation of unsaturated OVOCs under highly complex pollution conditions. However, further ambient studies are required to investigate whether the findings presented here can be applied to other SOA precursors under different environmental conditions.

■ ASSOCIATED CONTENT

Supporting Information

The Supporting Information is available free of charge on the ACS Publications website at DOI: 10.1021/acs.est.9b02702.

Table S1and S2, Figures S1−S9, and kinetic model reactions of BVE ozonolysis (PDF)

■ AUTHOR INFORMATION

Corresponding Author

*Phone: (+86)-010-62849123. E-mail: honghe @rcees.ac.cn.

ORCID

Peng Zhang: 0000-0002-0620-7673
Tianzeng Chen: 0000-0001-8123-0534
Jun Liu: 0000-0002-3065-799X
Changgeng Liu: 0000-0002-4899-0985
Jinzhu Ma: 0000-0003-1878-0669
Qingxin Ma: 0000-0002-9668-7008
Biwu Chu: 0000-0002-7548-5669

Notes

The authors declare no competing financial interest.

■ ACKNOWLEDGMENTS

This work was financially supported by the National Key R&D Program of China (2016YFC0202700, 2018YFC0506901), National Natural Science Foundation of China (41605100, 21876185, 91744205, 41877304, 41705134), and Youth Innovation Promotion Association, CAS (2018055, 2017064).

■ REFERENCES

(1) Kanakidou, M.; Seinfeld, J. H.; Pandis, S. N.; Barnes, I.; Dentener, F. J.; Facchini, M. C.; Van Dingenen, R.; Ervens, B.; Nenes, A.; Nielsen, C. J.; Swietlicki, E.; Putaud, J. P.; Balkanski, Y.; Fuzzi, S.; Horth, J.; Moortgat, G. K.; Winterhalter, R.; Myhre, C. E. L.; Tsigaridis, K.; Vignati, E.; Stephanou, E. G.; Wilson, J. Organic aerosol and global climate modelling: a review. *Atmos. Chem. Phys.* **2005**, *5*, 1053−1123.

(2) Zhang, Q.; Jimenez, J. L.; Canagaratna, M. R.; Allan, J. D.; Coe, H.; Ulbrich, I.; Alfarra, M. R.; Takami, A.; Middlebrook, A. M.; Sun, Y. L.; Dzepina, K.; Dunlea, E.; Docherty, K.; DeCarlo, P. F.; Salcedo, D.; Onasch, T.; Jayne, J. T.; Miyoshi, T.; Shimono, A.; Hatakeyama, S.; Takegawa, N.; Kondo, Y.; Schneider, J.; Drewnick, F.; Borrmann, S.; Weimer, S.; Demerjian, K.; Williams, P.; Bower, K.; Bahreini, R.; Cottrell, L.; Griffin, R. J.; Rautiainen, J.; Sun, J. Y.; Zhang, Y. M.; Worsnop, D. R. Ubiquity and dominance of oxygenated species in organic aerosols in anthropogenically-influenced Northern Hemisphere midlatitudes. *Geophys. Res. Lett.* **2007**, *34* (13), L13801.

(3) Dzepina, K.; Volkamer, R. M.; Madronich, S.; Tulet, P.; Ulbrich, I. M.; Zhang, Q.; Cappa, C. D.; Ziemann, P. J.; Jimenez, J. L. Evaluation of recently-proposed secondary organic aerosol models for a case study in Mexico City. *Atmos. Chem. Phys.* **2009**, *9* (15), 5681−5709.

(4) Cappa, C. D.; Jathar, S. H.; Kleeman, M. J.; Docherty, K. S.; Jimenez, J. L.; Seinfeld, J. H.; Wexler, A. S. Simulating secondary organic aerosol in a regional air quality model using the statistical oxidation model - Part 2: Assessing the influence of vapor wall losses. *Atmos. Chem. Phys.* **2016**, *16* (5), 3041−3059.

(5) Heald, C. L.; Jacob, D. J.; Park, R. J.; Russell, L. M.; Huebert, B. J.; Seinfeld, J. H.; Liao, H.; Weber, R. J. A large organic aerosol source in the free troposphere missing from current models. *Geophys. Res. Lett.* **2005**, DOI: 10.1029/2005GL023831.

(6) Ensberg, J. J.; Hayes, P. L.; Jimenez, J. L.; Gilman, J. B.; Kuster, W. C.; de Gouw, J. A.; Holloway, J. S.; Gordon, T. D.; Jathar, S.; Robinson, A. L.; Seinfeld, J. H. Emission factor ratios, SOA mass yields, and the impact of vehicular emissions on SOA formation. *Atmos. Chem. Phys.* **2014**, *14* (5), 2383−2397.

(7) Volkamer, R.; Jimenez, J. L.; San Martini, F.; Dzepina, K.; Zhang, Q.; Salcedo, D.; Molina, L. T.; Worsnop, D. R.; Molina, M. J. Secondary organic aerosol formation from anthropogenic air pollution: Rapid and higher than expected. *Geophys. Res. Lett.* **2006**, *33* (17), L17811.

(8) Li, S. M.; Leithead, A.; Moussa, S. G.; Liggio, J.; Moran, M. D.; Wang, D.; Hayden, K.; Darlington, A.; Gordon, M.; Staebler, R.; Makar, P. A.; Stroud, C. A.; McLaren, R.; Liu, P. S. K.; O'Brien, J.; Mittermeier, R. L.; Zhang, J. H.; Marson, G.; Cober, S. G.; Wolde, M.; Wentzell, J. J. B. Differences between measured and reported volatile organic compound emissions from oil sands facilities in Alberta, Canada. *Proc. Natl. Acad. Sci. USA* **2017**, *114* (19), E3756−E3765.

(9) De Haan, D. O.; Corrigan, A. L.; Tolbert, M. A.; Jimenez, J. L.; Wood, S. E.; Turley, J. J. Secondary organic aerosol formation by self-reactions of methylglyoxal and glyoxal in evaporating droplets. *Environ. Sci. Technol.* **2009**, *43* (21), 8184−8190.

(10) Lim, Y. B.; Tan, Y.; Turpin, B. J. Chemical insights, explicit chemistry, and yields of secondary organic aerosol from OH radical oxidation of methylglyoxal and glyoxal in the aqueous phase. *Atmos. Chem. Phys.* **2013**, *13* (17), 8651−8667.

(11) Ervens, B.; Turpin, B. J.; Weber, R. J. Secondary organic aerosol formation in cloud droplets and aqueous particles (aqSOA): a review of laboratory, field and model studies. *Atmos. Chem. Phys.* **2011**, *11* (21), 11069−11102.

(12) Hu, J. L.; Wang, P.; Ying, Q.; Zhang, H. L.; Chen, J. J.; Ge, X. L.; Li, X. H.; Jiang, J. K.; Wang, S. X.; Zhang, J.; Zhao, Y.; Zhang, Y. Y. Modeling biogenic and anthropogenic secondary organic aerosol in China. *Atmos. Chem. Phys.* **2017**, *17* (1), 77−92.

(13) Mellouki, A.; Wallington, T. J.; Chen, J. Atmospheric Chemistry of Oxygenated Volatile Organic Compounds: Impacts on Air Quality and Climate. *Chem. Rev.* **2015**, *115* (10), 3984−4014.

(14) Klotz, B.; Barnes, I.; Imamura, T. Product study of the gas-phase reactions of O_3, OH and NO_3 radicals with methyl vinyl ether. *Phys. Chem. Chem. Phys.* **2004**, *6* (8), 1725−1734.

(15) Grosjean, E.; Grosjean, D. The gas phase reaction of unsaturated oxygenates with ozone: Carbonyl products and comparison with the alkene-ozone reaction. *J. Atmos. Chem.* **1997**, *27* (3), 271−289.

(16) Zhou, S. M.; Barnes, I.; Zhu, T.; Benter, T. Rate coefficients for the gas-phase reactions of OH and NO_3 Radicals and O_3 with ethyleneglycol monovinyl ether, ethyleneglycol divinyl ether, and

DOI: 10.1021/acs.est.9b02702
Environ. Sci. Technol. 2019, 53, 8845−8853

diethyleneglycol divinyl ether. *J. Phys. Chem. A* **2009**, *113* (5), 858−865.
(17) Zhou, S. M.; Barnes, I.; Zhu, T.; Bejan, I.; Benter, T. Kinetic study of the gas-phase reactions of OH and NO_3 radicals and O_3 with selected vinyl ethers. *J. Phys. Chem. A* **2006**, *110* (23), 7386−7392.
(18) Thiault, G.; Thevenet, R.; Mellouki, A.; Le Bras, G. OH and O_3-initiated oxidation of ethyl vinyl ether. *Phys. Chem. Chem. Phys.* **2002**, *4* (4), 613−619.
(19) Sadezky, A.; Chaimbault, P.; Mellouki, A.; Rompp, A.; Winterhalter, R.; Le Bras, G.; Moortgat, G. K. Formation of secondary organic aerosol and oligomers from the ozonolysis of enol ethers. *Atmos. Chem. Phys.* **2006**, *6*, 5009−5024.
(20) Sadezky, A.; Winterhalter, R.; Kanawati, B.; Rompp, A.; Spengler, B.; Mellouki, A.; Le Bras, G.; Chaimbault, P.; Moortgat, G. K. Oligomer formation during gas-phase ozonolysis of small alkenes and enol ethers: new evidence for the central role of the Criegee Intermediate as oligomer chain unit. *Atmos. Chem. Phys.* **2008**, *8* (10), 2667−2699.
(21) Ye, J. H.; Abbatt, J. P. D.; Chan, A. W. H. Novel pathway of SO_2 oxidation in the atmosphere: reactions with monoterpene ozonolysis intermediates and secondary organic aerosol. *Atmos. Chem. Phys.* **2018**, *18* (8), 5549−5565.
(22) Chu, B.; Zhang, X.; Liu, Y.; He, H.; Sun, Y.; Jiang, J.; Li, J.; Hao, J. Synergetic formation of secondary inorganic and organic aerosol: effect of SO_2 and NH_3 on particle formation and growth. *Atmos. Chem. Phys.* **2016**, *16* (22), 14219−14230.
(23) Friedman, B.; Brophy, P.; Brune, W. H.; Farmer, D. K. Anthropogenic sulfur perturbations on biogenic oxidation: SO_2 additions impact gas-phase OH oxidation products of α-and β-pinene. *Environ. Sci. Technol.* **2016**, *50* (3), 1269−1279.
(24) Chen, T.; Liu, Y.; Ma, Q.; Chu, B.; Zhang, P.; Liu, C.; Liu, J.; He, H. Significant source of secondary aerosol: formation from gasoline evaporative emissions in the presence of SO_2 and NH_3. *Atmos. Chem. Phys.* **2019**, *19* (12), 8063−8081.
(25) Newland, M. J.; Rickard, A. R.; Vereecken, L.; Muñoz, A.; Ródenas, M.; Bloss, W. J. Atmospheric isoprene ozonolysis: impacts of stabilised Criegee intermediate reactions with SO_2, H_2O and dimethyl sulfide. *Atmos. Chem. Phys.* **2015**, *15* (16), 9521−9536.
(26) Sipila, M.; Jokinen, T.; Berndt, T.; Richters, S.; Makkonen, R.; Donahue, N. M.; Mauldin, R. L.; Kurten, T.; Paasonen, P.; Sarnela, N.; Ehn, M.; Junninen, H.; Rissanen, M. P.; Thornton, J.; Stratmann, F.; Herrmann, H.; Worsnop, D. R.; Kulmala, M.; Kerminen, V. M.; Petaja, T. Reactivity of stabilized Criegee intermediates (sCIs) from isoprene and monoterpene ozonolysis toward SO_2 and organic acids. *Atmos. Chem. Phys.* **2014**, *14* (22), 12143−12153.
(27) Zhang, H.; Worton, D. R.; Lewandowski, M.; Ortega, J.; Rubitschun, C. L.; Park, J.-H.; Kristensen, K.; Campuzano-Jost, P.; Day, D. A.; Jimenez, J. L. Organosulfates as tracers for secondary organic aerosol (SOA) formation from 2-methyl-3-buten-2-ol (MBO) in the atmosphere. *Environ. Sci. Technol.* **2012**, *46* (17), 9437−9446.
(28) Shalamzari, M. S.; Vermeylen, R.; Blockhuys, F.; Kleindienst, T. E.; Lewandowski, M.; Szmigielski, R.; Rudzinski, K. J.; Spólnik, G.; Danikiewicz, W.; Maenhaut, W. Characterization of polar organosulfates in secondary organic aerosol from the unsaturated aldehydes 2-E-pentenal, 2-E-hexenal, and 3-Z-hexenal. *Atmos. Chem. Phys.* **2016**, *16* (11), 7135−7148.
(29) Liu, C. G.; Chen, T. Z.; Liu, Y. C.; Liu, J.; He, H.; Zhang, P. Enhancement of secondary organic aerosol formation and its oxidation state by SO_2 during photooxidation of 2-methoxyphenol. *Atmos. Chem. Phys.* **2019**, *19* (4), 2687−2700.
(30) Liu, J.; Chu, B.; Chen, T.; et al. Secondary organic aerosol formation from ambient air at an urban site in Beijing: effects of OH exposure and precursor concentratio. *Environ. Sci. Technol.* **2018**, *52* (12), 6834−6841.
(31) Canagaratna, M. R.; Jayne, J. T.; Jimenez, J. L.; Allan, J. D.; Alfarra, M. R.; Zhang, Q.; Onasch, T. B.; Drewnick, F.; Coe, H.; Middlebrook, A.; Delia, A.; Williams, L. R.; Trimborn, A. M.; Northway, M. J.; DeCarlo, P. F.; Kolb, C. E.; Davidovits, P.; Worsnop, D. R. Chemical and microphysical characterization of ambient aerosols with the aerodyne aerosol mass spectrometer. *Mass. Spectrom. Rev.* **2007**, *26* (2), 185−222.
(32) DeCarlo, P. F.; Kimmel, J. R.; Trimborn, A.; Northway, M. J.; Jayne, J. T.; Aiken, A. C.; Gonin, M.; Fuhrer, K.; Horvath, T.; Docherty, K. S.; Worsnop, D. R.; Jimenez, J. L. Field-deployable, high-resolution, time-of-flight aerosol mass spectrometer. *Anal. Chem.* **2006**, *78* (24), 8281−8289.
(33) Chen, T. Z.; Liu, Y. C.; Chu, B. W.; Liu, C. G.; Liu, J.; Ge, Y. L.; Ma, Q. X.; Ma, J. Z.; He, H. Differences of the oxidation process and secondary organic aerosol formation at low and high precursor concentrations. *J. Environ. Sci.* **2019**, *79*, 256−263.
(34) Takekawa, H.; Minoura, H.; Yamazaki, S. Temperature dependence of secondary organic aerosol formation by photo-oxidation of hydrocarbons. *Atmos. Environ.* **2003**, *37* (24), 3413−3424.
(35) Bauduin, S.; Clarisse, L.; Hadji-Lazaro, J.; Theys, N.; Clerbaux, C.; Coheur, P. F. Retrieval of near-surface sulfur dioxide (SO_2) concentrations at a global scale using IASI satellite observations. *Atmos. Meas. Tech.* **2016**, *9* (2), 721−740.
(36) Wang, L. W.; Wen, L.; Xu, C. H.; Chen, J. M.; Wang, X. F.; Yang, L. X.; Wang, W. X.; Yang, X.; Sui, X.; Yao, L.; Zhang, Q. Z. HONO and its potential source particulate nitrite at an urban site in North China during the cold season. *Sci. Total. Environ.* **2015**, *538*, 93−101.
(37) Zhang, Q.; Shen, Z. X.; Cao, J. J.; Zhang, R. J.; Zhang, L. M.; Huang, R. J.; Zheng, C. J.; Wang, L. Q.; Liu, S. X.; Xu, H. M.; Zheng, C. L.; Liu, P. P. Variations in PM2.5, TSP, BC, and trace gases (NO_2, SO_2, and O_3) between haze and non-haze episodes in winter over Xi'an, China. *Atmos. Environ.* **2015**, *112*, 64−71.
(38) Kundu, S.; Fisseha, R.; Putman, A. L.; Rahn, T. A.; Mazzoleni, L. R. High molecular weight SOA formation during limonene ozonolysis: insights from ultrahigh-resolution FT-ICR mass spectrometry characterization. *Atmos. Chem. Phys.* **2012**, *12* (12), 5523−5536.
(39) Kundu, S.; Fisseha, R.; Putman, A. L.; Rahn, T. A.; Mazzoleni, L. High molecular weight SOA formation during limonene ozonolysis: insights from ultrahigh-resolution FT-ICR mass spectrometry characterization. *Atmos. Chem. Phys.* **2012**, *12* (12), 5523−5536.
(40) Van Wyngarden, A. L.; Perez-Montano, S.; Bui, J. V. H.; Li, E. S. W.; Nelson, T. E.; Ha, K. T.; Leong, L.; Iraci, L. T. Complex chemical composition of colored surface films formed from reactions of propanal in sulfuric acid at upper troposphere/lower stratosphere aerosol acidities. *Atmos. Chem. Phys.* **2015**, *15* (8), 4225−4239.
(41) Sipila, M.; Berndt, T.; Petaja, T.; Brus, D.; Vanhanen, J.; Stratmann, F.; Patokoski, J.; Mauldin, R. L., III; Hyvarinen, A.-P.; Lihavainen, H.; Kulmala, M. The role of sulfuric acid in atmospheric nucleation. *Science* **2010**, *327* (5970), 1243−1246.
(42) Sihto, S. L.; Kulmala, M.; Kerminen, V. M.; Dal Maso, M.; Petaja, T.; Riipinen, I.; Korhonen, H.; Arnold, F.; Janson, R.; Boy, M.; Laaksonen, A.; Lehtinen, K. E. J. Atmospheric sulphuric acid and aerosol formation: implications from atmospheric measurements for nucleation and early growth mechanisms. *Atmos. Chem. Phys.* **2006**, *6*, 4079−4091.
(43) Xiao, S.; Wang, M. Y.; Yao, L.; Kulmala, M.; Zhou, B.; Yang, X.; Chen, J. M.; Wang, D. F.; Fu, Q. Y.; Worsnop, D. R.; Wang, L. Strong atmospheric new particle formation in winter in urban Shanghai, China. *Atmos. Chem. Phys.* **2015**, *15* (4), 1769−1781.
(44) Li, Y. J.; Lee, B. Y. L.; Yu, J. Z.; Ng, N. L.; Chan, C. K. Evaluating the degree of oxygenation of organic aerosol during foggy and hazy days in Hong Kong using high-resolution time-of-flight aerosol mass spectrometry (HR-ToF-AMS). *Atmos. Chem. Phys.* **2013**, *13* (17), 8739−8753.
(45) Ng, N. L.; Canagaratna, M. R.; Jimenez, J. L.; Chhabra, P. S.; Seinfeld, J. H.; Worsnop, D. R. Changes in organic aerosol composition with aging inferred from aerosol mass spectra. *Atmos. Chem. Phys.* **2011**, *11* (13), 6465−6474.
(46) Heald, C. L.; Kroll, J. H.; Jimenez, J. L.; Docherty, K. S.; DeCarlo, P. F.; Aiken, A. C.; Chen, Q.; Martin, S. T.; Farmer, D. K.;

DOI: 10.1021/acs.est.9b02702
Environ. Sci. Technol. 2019, 53, 8845−8853

Artaxo, P. A simplified description of the evolution of organic aerosol composition in the atmosphere. *Geophys. Res. Lett.* **2010**, *37*, L08803.
(47) Zhao, D.; Kaminski, M.; Schlag, P.; Fuchs, H.; Acir, I.-H.; Bohn, B.; Häseler, R.; Kiendler-Scharr, A.; Rohrer, F.; Tillmann, R. Secondary organic aerosol formation from hydroxyl radical oxidation and ozonolysis of monoterpenes. *Atmos. Chem. Phys.* **2015**, *15* (2), 991−1012.
(48) Cappa, C. D.; Zhang, X.; Loza, C. L.; Craven, J. S.; Yee, L. D.; Seinfeld, J. H. Application of the Statistical Oxidation Model (SOM) to Secondary Organic Aerosol formation from photooxidation of C_{12} alkanes. *Atmos. Chem. Phys.* **2013**, *13* (3), 1591−1606.
(49) Canagaratna, M. R.; Jimenez, J. L.; Kroll, J. H.; Chen, Q.; Kessler, S. H.; Massoli, P.; Hildebrandt Ruiz, L.; Fortner, E.; Williams, L. R.; Wilson, K. R.; Surratt, J. D.; Donahue, N. M.; Jayne, J. T.; Worsnop, D. R. Elemental ratio measurements of organic compounds using aerosol mass spectrometry: characterization, improved calibration, and implications. *Atmos. Chem. Phys.* **2015**, *15* (1), 253−272.
(50) Kroll, J. H.; Donahue, N. M.; Jimenez, J. L.; Kessler, S. H.; Canagaratna, M. R.; Wilson, K. R.; Altieri, K. E.; Mazzoleni, L. R.; Wozniak, A. S.; Bluhm, H.; Mysak, E. R.; Smith, J. D.; Kolb, C. E.; Worsnop, D. R. Carbon oxidation state as a metric for describing the chemistry of atmospheric organic aerosol. *Nat. Chem.* **2011**, *3* (2), 133−139.
(51) Huang, D. D.; Li, Y. J.; Lee, B. P.; Chan, C. K. Analysis of organic sulfur compounds in atmospheric aerosols at the HKUST supersite in Hong Kong using HR-ToF-AMS. *Environ. Sci. Technol.* **2015**, *49* (6), 3672−3679.
(52) Hinks, M. L.; Montoya-Aguilera, J.; Ellison, L.; Lin, P.; Laskin, A.; Laskin, J.; Shiraiwa, M.; Dabdub, D.; Nizkorodov, S. A. Effect of relative humidity on the composition of secondary organic aerosol from the oxidation of toluene. *Atmos. Chem. Phys.* **2018**, *18* (3), 1643−1652.
(53) Poulain, L.; Wu, Z.; Petters, M. D.; Wex, H.; Hallbauer, E.; Wehner, B.; Massling, A.; Kreidenweis, S. M.; Stratmann, F. Towards closing the gap between hygroscopic growth and CCN activation for secondary organic aerosols - Part 3: Influence of the chemical composition on the hygroscopic properties and volatile fractions of aerosols. *Atmos. Chem. Phys.* **2010**, *10* (8), 3775−3785.
(54) Heine, N.; Arata, C.; Goldstein, A. H.; Houle, F. A.; Wilson, K. R. Multiphase mechanism for the production of sulfuric acid from SO_2 by Criegee Intermediates formed during the heterogeneous reaction of ozone with squalene. *J. Phys. Chem. Lett.* **2018**, *9* (12), 3504−3510.
(55) Zhang, R. Y.; Suh, I.; Zhao, J.; Zhang, D.; Fortner, E. C.; Tie, X. X.; Molina, L. T.; Molina, M. J. Atmospheric new particle formation enhanced by organic acids. *Science* **2004**, *304* (5676), 1487−1490.
(56) Berndt, T.; Stratmann, F.; Sipila, M.; Vanhanen, J.; Petaja, T.; Mikkila, J.; Gruner, A.; Spindler, G.; Mauldin, R. L.; Curtius, J.; Kulmala, M.; Heintzenberg, J. Laboratory study on new particle formation from the reaction OH + SO_2: influence of experimental conditions, H_2O vapour, NH_3 and the amine tert-butylamine on the overall process. *Atmos. Chem. Phys.* **2010**, *10* (15), 7101−7116.
(57) Nguyen, T. B.; Roach, P. J.; Laskin, J.; Laskin, A.; Nizkorodov, S. A. Effect of humidity on the composition of isoprene photooxidation secondary organic aerosol. *Atmos. Chem. Phys.* **2011**, *11* (14), 6931−6944.
(58) Jonsson, A. M.; Hallquist, M.; Ljungstrom, E. Impact of humidity on the ozone initiated oxidation of limonene, Δ^3-carene, and α-pinene. *Environ. Sci. Technol.* **2006**, *40* (1), 188−194.
(59) Huang, H. L.; Chao, W.; Lin, J. J. M. Kinetics of a Criegee intermediate that would survive high humidity and may oxidize atmospheric SO_2. *Proc. Natl. Acad. Sci. U. S. A.* **2015**, *112* (35), 10857−10862.
(60) Chao, W.; Hsieh, J. T.; Chang, C. H.; Lin, J. J. M. Direct kinetic measurement of the reaction of the simplest Criegee intermediate with water vapor. *Science* **2015**, *347* (6223), 751−754.
(61) Seinfeld, J. H.; Pandis, S. N. *Atmospheric chemistry and physics: from air pollution to climate change*; John Wiley & Sons, 2016.
(62) Berndt, T.; Voigtländer, J.; Stratmann, F.; Junninen, H.; Mauldin, R. L., III; Sipilä, M.; Kulmala, M.; Herrmann, H. Competing atmospheric reactions of CH_2OO with SO_2 and water vapour. *Phys. Chem. Chem. Phys.* **2014**, *16* (36), 19130−19136.
(63) Berndt, T.; Jokinen, T.; Sipilä, M.; Mauldin, R. L., III; Herrmann, H.; Stratmann, F.; Junninen, H.; Kulmala, M. H_2SO_4 formation from the gas-phase reaction of stabilized Criegee Intermediates with SO_2: Influence of water vapour content and temperature. *Atmos. Environ.* **2014**, *89*, 603−612.
(64) Huang, H.-L.; Chao, W. Kinetics of a Criegee intermediate that would survive high humidity and may oxidize atmospheric SO_2. *P. Natl. Acad. Sci. USA* **2015**, *112* (35), 10857−10862.
(65) Berndt, T.; Voigtlander, J.; Stratmann, F.; Junninen, H.; Mauldin, R. L.; Sipila, M.; Kulmala, M.; Herrmann, H. Competing atmospheric reactions of CH_2OO with SO_2 and water vapour. *Phys. Chem. Chem. Phys.* **2014**, *16* (36), 19130−19136.
(66) Zhang, H.; Surratt, J. D.; Lin, Y. H.; Bapat, J.; Kamens, R. M. Effect of relative humidity on SOA formation from isoprene/NO photooxidation: enhancement of 2-methylglyceric acid and its corresponding oligoesters under dry conditions. *Atmos. Chem. Phys.* **2011**, *11* (13), 6411−6424.
(67) Kristensen, K.; Cui, T.; Zhang, H.; Gold, A.; Glasius, M.; Surratt, J. D. Dimers in alpha-pinene secondary organic aerosol: effect of hydroxyl radical, ozone, relative humidity and aerosol acidity. *Atmos. Chem. Phys.* **2014**, *14* (8), 4201−4218.
(68) Volkamer, R.; Ziemann, P. J.; Molina, M. J. Secondary Organic Aerosol Formation from Acetylene (C_2H_2): seed effect on SOA yields due to organic photochemistry in the aerosol aqueous phase. *Atmos. Chem. Phys.* **2009**, *9* (6), 1907−1928.
(69) Lambe, A. T.; Chhabra, P. S.; Onasch, T. B.; Brune, W. H.; Hunter, J. F.; Kroll, J. H.; Cummings, M. J.; Brogan, J. F.; Parmar, Y.; Worsnop, D. R.; Kolb, C. E.; Davidovits, P. Effect of oxidant concentration, exposure time, and seed particles on secondary organic aerosol chemical composition and yield. *Atmos. Chem. Phys.* **2015**, *15* (6), 3063−3075.
(70) Offenberg, J. H.; Lewandowski, M.; Edney, E. O.; Kleindienst, T. E.; Jaoui, M. Influence of aerosol acidity on the formation of secondary organic aerosol from biogenic precursor hydrocarbons. *Environ. Sci. Technol.* **2009**, *43* (20), 7742−7747.
(71) Surratt, J. D.; Lewandowski, M.; Offenberg, J. H.; Jaoui, M.; Kleindienst, T. E.; Edney, E. O.; Seinfeld, J. H. Effect of acidity on secondary organic aerosol formation from isoprene. *Environ. Sci. Technol.* **2007**, *41* (15), 5363−5369.
(72) Liggio, J.; Li, S. M. Reversible and irreversible processing of biogenic olefins on acidic aerosols. *Atmos. Chem. Phys.* **2008**, *8* (7), 2039−2055.
(73) Surratt, J. D.; Gomez-Gonzalez, Y.; Chan, A. W. H.; Vermeylen, R.; Shahgholi, M.; Kleindienst, T. E.; Edney, E. O.; Offenberg, J. H.; Lewandowski, M.; Jaoui, M.; Maenhaut, W.; Claeys, M.; Flagan, R. C.; Seinfeld, J. H. Organosulfate formation in biogenic secondary organic aerosol. *J. Phys. Chem. A* **2008**, *112* (36), 8345−8378.
(74) Tolocka, M. P.; Jang, M.; Ginter, J. M.; Cox, F. J.; Kamens, R. M.; Johnston, M. V. Formation of oligomers in secondary organic aerosol. *Environ. Sci. Technol.* **2004**, *38* (5), 1428−1434.

DOI: 10.1021/acs.est.9b02702
Environ. Sci. Technol. 2019, 53, 8845−8853